

Article

Sand Transport and Deposition Behaviour in Subsea Pipelines for Flow Assurance

Yan Yang ¹, Haoping Peng ¹ and Chuang Wen ^{2,*} 

¹ School of Petroleum Engineering, Changzhou University, Wujin District, Changzhou 213164, China; yyan-petroleum@cczu.edu.cn (Y.Y.); penghp@cczu.edu.cn (H.P.)

² Department of Mechanical Engineering, Technical University of Denmark, Nils Koppels Allé, 2800 Kgs. Lyngby, Denmark

* Correspondence: cwen@mek.dtu.dk

Received: 5 October 2019; Accepted: 23 October 2019; Published: 25 October 2019



Abstract: Sand transport through tubing and pipeline could cause a series of problems to flow assurance, if not properly managed or controlled. The most serious problem is the accumulation and erosion in multiphase flow pipelines and the surface equipment. Therefore, the importance of understanding the transport and deposition behaviour of sands through multiphase flow pipelines cannot be overemphasized. This study presents the sand transport and deposition characteristics in the complicated multiphase flow pipeline. The numerical result shows that the slurry velocity presents a uniform distribution in the multiphase flow pipeline at the sand concentration of 5% and the sand diameter of 50 μm . However, the slurry velocity at the bottom of the pipeline is significantly smaller than that at the top when the sand concentration and diameter reach 30% and 300 μm , respectively. It indicates that the sand deposition at the bottom of the pipe declines the slurry velocity and transport capacity. The deposition thickness is approximately 10% of the pipe diameter even at the low concentration of 5% sand with a small sand diameter of 50 μm and a high slurry velocity of 1.8 m/s. The sand deposition reaches about 30% of the pipe diameter at the same low concentration and high slurry velocity when the sand diameter increases to 300 μm .

Keywords: sand transport; deposition; liquid-solid two-phase flow; particle flow; pipeline; flow assurance

1. Introduction

The demand for energy supply is a key issue for the global economy. The petroleum supply plays an important role in primary energy. In the petroleum supply networks, sand transport is generally a severe problem for most oil and gas reservoirs all over the world [1–3]. It is more important especially for the subsea production systems considering the flow assurance. The deposition of solid sand in the pipe bottom and equipment can cause a series of risks. For instance, the formation of the sand bed in the pipeline decreases the flow area and correspondingly increases the frictional pressure losses. Moreover, sand transport can cause erosion and corrosion problems as a result of the impact on the pipe wall and the microbial attack under the sand bed. In addition, the slurry flow containing sands could lead to equipment failure. Therefore, the deposition and transport of the sand in slurry flows attract much attention, and it is also a very significant issue in the petroleum industry.

A series of computer-controlled experiments were conducted in a thin fluid (like water) and the key parameter distribution was obtained at various flow rates, injected sand concentrations, and fluid viscosities [4–6]. Doron et al. [7] experimentally studied the transport behaviour of the coarse solids in a horizontal pipeline. Gillies and Shook [8] employed the traversing gamma-ray gauges to measure the sand concentration in a horizontal pipeline with coarse solids nominally from 180 to 2400 μm .

Their results indicated that the maximal concentration gradient (0.47 in their studies) was irrelevant to the mean velocity. Gillies et al. [9] experimentally studied the sand transport characteristics in a horizontal pipeline with viscous Newtonian fluids. Their results showed that a pressure gradient of 2 kPa/m was required to transport sand in laminar flow. Kaushal et al. [10–13] conducted a series of experiments to study the sand transport characteristic in multiphase flow pipelines. The measurement of the pressure drop and concentration was experimentally observed in the liquid-solid slurry flow. Duan et al. [14] investigated experimentally the critical resuspension velocity and the critical deposition velocity for different size sands in slurry flows. It indicated that the critical resuspension velocity was two to three times smaller than the critical deposition velocity. Najmi et al. [15] experimentally studied the critical flow rate of gas and liquid to keep particles moving in a horizontal pipeline in stratified and intermittent flow with a small liquid hold-up of about 0.02. The volume fraction of the solid phase (0.01–0.1%) was experimentally measured in a horizontal pipeline at a very low concentration. Rice et al. [16] utilized two kinds of particles including the glass and plastic solids to understand the sand transport behaviour in the multiphase flow pipeline.

A computational model was developed by Roco and Shook [17] to predict the quasi-uniform slurry flow with the range of sand volume concentration below 40%. Their simulated results of concentration and velocity were compared with experimental data and showed a good agreement. The sand transport process was investigated in a horizontal well by means of numerical simulations [18]. Ebadian et al. [19,20] developed an algebraic slip mixture model to predict the sand transport behaviour within a horizontal pipeline. Their comparison of the pressure drop between the computational and experimental results showed a good agreement. Danielson [21] considered the slip velocity to develop a two-fluid model for the slurry flows, and a good agreement between the simulation and experiment was obtained in the sand bed height. An analytical near-wall model was developed to describe the liquid-solid two-phase flow, and the numerical result showed a good agreement with the experimental concentration [22]. A two-fluid model was proposed to predict the fully suspended slurry flow, and it was validated by experimental data [23–25]. In another study, they proposed an improved mathematical model for the slurry flow within a horizontal pipeline [26]. The comparison between the simulation and experiment showed that the new model was more accurate than the previous one. Hadinoto [27] adapted the two-fluid flow model to predict the turbulence modulation characteristic in a vertical pipeline at a low solid volume fraction from 0.5% to 4.0%. The numerical and experimental results showed that the drag correlation significantly affected the accuracy of the computational fluid dynamics (CFD simulation). The Euler-granular model was employed by Kaushal et al. [28] to predict the sand transport behaviour in a horizontal pipeline with fine particles at high concentrations. The concentration distributions of the numerical and experimental results were in good agreement. Soepyan et al. [29] developed a CFD model to predict the fluid velocity of the slurry flow in a horizontal pipeline at a low concentration by volume. Table 1 lists recent studies on sand transport and deposition in multiphase flow pipelines with a focus on low concentration conditions. These studies demonstrated the importance of the effect of sands on the flow process even in low concentrations for multiphase flow pipelines.

Table 1. Recent studies on sand transport and deposition in multiphase flow pipelines with a focus on low concentration conditions.

References	Sand Size (μm)	Sand Concentration (%)	Pipe Diameter (mm)
Dabirian et al. 2016 [30]	45–600	0.025–1%	97
Najmi et al. 2016 [31]	20–300	0–1%	50
Najmi et al. 2016 [32]	150–300	0.01–0.1%	50–100
Dabirian et al. 2018 [33]	150–600	0–1%	50
Dabirian et al. 2018 [34]	45–600	0.025–1%	97
Tebowei et al. 2018 [35]	255	0.04%	100
Fajemidupe et al. 2019 [36]	212–800	0–0.006%	50.4
Leporini et al. 2019 [37]	100–1100	0.0065–0.056%	63
Leporini et al. 2019 [38]	45–600	0.00161–0.0538	50–100

The purpose of this study is to evaluate the transportation and deposition process of the sand in multiphase flows, which will contribute to the flow assurance of the subsea pipeline system. The novelty of this work includes understanding the sand transportation and deposition behaviour in multiphase flows under extreme conditions in a complicated pipeline system. This was done in this study with the aim to introduce a numerical simulation to predict the sand transport process with the sand concentration up to 30%. The effect of the particle size and velocity on the sand deposition were carried out with the Eulerian-Eulerian two-fluid model. The deposition and transport of sands are described in detail in different cross-sections of the multiphase flow pipeline, which contributes to the understanding of the flow behaviour of this liquid-solid two-phase flow system for oil and gas industry. The key contribution of this work can be summarized as (a) Development and application of a computational fluid dynamics modelling that captures the sand transport process in complex multiphase flow pipelines, (b) the baseline simulation result of liquid-sand two-phase flows have been validated against experimental data, (c) case studies for the effect of the particle size and the inlet velocity has been carried out with the detailed analysis of flow behaviour.

2. Numerical Approaches

2.1. Governing Equations

The Eulerian two-fluid model was employed to predict the sand transport behaviour in subsea multiphase flow pipelines. In this simulation, the continuous phase was assumed as a Newtonian fluid and the water was utilized as the working fluid. Correspondingly, the mass and the momentum conservation equations were solved individually as follows.

The conservation of mass equation for phase q is [39]:

$$\frac{\partial}{\partial t}(\alpha_q \rho_q) + \nabla \cdot (\alpha_q \rho_q \mathbf{u}_q) = \sum_{s=1}^n (\dot{m}_{sq} - \dot{m}_{qs}) \quad (1)$$

where α is the phase volume fraction, ρ_q is the physical density of phase q , \mathbf{u}_q is the velocity of phase q , \dot{m}_{sq} and \dot{m}_{qs} represents the mass transfer between the phase s and phase q . t is time.

The conservation of momentum equation for phase q is described as follows [39]:

$$\begin{aligned} \frac{\partial}{\partial t}(\alpha_q \rho_q \mathbf{u}_q) + \nabla \cdot (\alpha_q \rho_q \mathbf{u}_q \mathbf{u}_q) = & -\alpha_q \nabla p + \nabla \cdot \bar{\bar{\tau}}_q + \alpha_q \rho_q \mathbf{g} + \\ & + \sum_{s=1}^n (\mathbf{F}_{sq} + \dot{m}_{sq} \mathbf{u}_{sq} - \dot{m}_{qs} \mathbf{u}_{qs}) \\ & + (\mathbf{F}_q + \mathbf{F}_{lift,q} + \mathbf{F}_{wl,q} + \mathbf{F}_{um,q} + \mathbf{F}_{td,q}) \end{aligned} \quad (2)$$

where $\bar{\bar{\tau}}$ is the phase stress-strain tensor for phase q :

$$\bar{\bar{\tau}}_q = \alpha_q \mu_q (\nabla \mathbf{u}_q + \nabla \mathbf{u}_q^T) + \alpha_q \left(\lambda_q - \frac{2}{3} \mu_q \right) \nabla \cdot \mathbf{u}_q \bar{\mathbf{I}} \quad (3)$$

where \mathbf{g} is the acceleration of gravity, μ_q and λ_q are the shear and bulk viscosity of phase q , $\bar{\mathbf{I}}$ is unit tensor, \mathbf{F}^{sq} is an interaction force between phases, \mathbf{F}_q is an external body force, $\mathbf{F}_{lift,q}$ is a lift force, $\mathbf{F}_{wl,q}$ is a wall lubrication force, $\mathbf{F}_{vm,q}$ is a virtual mass force, and $\mathbf{F}_{td,q}$ is a turbulent dispersion force, p is the pressure shared by all phases. \mathbf{u}_{qs} and \mathbf{u}_{sq} are the interphase velocity.

The liquid-sand two-phase flow presents high turbulence because of the large velocity in multiphase flow pipelines. In this paper, the standard k - ε turbulence model was employed to solve the liquid-solid flow as a result of the robustness, economy, and reasonable accuracy. The turbulence kinetic energy, k , and its rate of dissipation, ε , are obtained from the following transport equations [39]:

$$\frac{\partial}{\partial t}(\rho k) + \frac{\partial}{\partial x_i}(\rho k u_i) = \frac{\partial}{\partial x_j} \left[\left(\mu + \frac{\mu_t}{\sigma_k} \right) \frac{\partial k}{\partial x_j} \right] + G_k + G_b - \rho \varepsilon - Y_M \quad (4)$$

$$\frac{\partial}{\partial t}(\rho\varepsilon) + \frac{\partial}{\partial x_i}(\rho\varepsilon u_i) = \frac{\partial}{\partial x_j} \left[\left(\mu + \frac{\mu_t}{\sigma_\varepsilon} \right) \frac{\partial \varepsilon}{\partial x_j} \right] + C_{1\varepsilon} \frac{\varepsilon}{k} (G_k + C_{3\varepsilon} G_b) - C_{2\varepsilon} \rho \frac{\varepsilon^2}{k} \quad (5)$$

$$\mu_t = \rho C_\mu \frac{k^2}{\varepsilon} \quad (6)$$

where G_k is the generation of turbulence kinetic energy due to the mean velocity gradients, G_b represents the generation of turbulence kinetic energy due to buoyancy, Y_M represents the contribution of the fluctuating dilatation in compressible turbulence to the overall dissipation rate. where C_μ , $C_{\varepsilon 1}$, $C_{\varepsilon 2}$ and $C_{\varepsilon 3}$ are constants. σ_k and σ_ε are the turbulent Prandtl numbers for k and ε , respectively. μ_t is the turbulent viscosity.

2.2. Numerical Schemes

The ANSYS FLUENT [39] software was used as a computational platform for the numerical study. The Eulerian multiphase flow model was employed to calculate the liquid-solid flow. The water (liquid) is the primary phase while the sand (solid) is the secondary phase in this study. The pressure-velocity coupling we used was the phase-coupled SIMPLE algorithm. The continuity equation, momentum equations, and turbulence equations were discretized with the second-order upwind scheme [40,41].

The numerical simulation was conducted in a horizontal pipeline. The pipe diameter and length were 200 mm and 8000 mm, respectively. The structured mesh was employed for the numerical study. The pipe geometry and grid system were shown in Figure 1. The fine mesh near the wall region was generated for exactly capturing the sand deposition and transport information. The velocity and outflow conditions were assigned to the pipe inlet and outlet, respectively. During the simulation, the following error formula is used to estimate the rightness of calculations and has been added in the revised manuscript.

$$R^\phi = \frac{\sum_{\text{cells } P} |\sum_{\text{nb}} a_{\text{nb}} \phi_{\text{nb}} + b - a_P \phi_P|}{\sum_{\text{cells } P} |a_P \phi_P|} \quad (7)$$

where ϕ is a general variable, P is the computational cell, R^ϕ is the computational residual, a_P is the centre coefficient, a_{nb} is the influence coefficient for the neighbouring cell, and b is the contribution of the constant part of the source term.

The resolution of the grid is a significant factor to influence the numerical result during the computational study of the sand transport and deposition in multiphase flow pipelines. The coarse mesh of 121,080 cells, the medium mesh of 203,490 cells and the fine mesh of 466,820 cells were employed here to test the sensitivity of the grid resolution on the numerical simulation. The slurry velocity at the cross-section of 20 times the pipe diameter was selected as a rational parameter to evaluate the effect of the grid resolution on the flow behaviour. The comparison results were shown in Figure 2 and Table 2, respectively. From the contours of the slurry velocity in Figure 2, it can be observed that these three different mesh cells predict almost the same distribution of the slurry velocity at the cross-section of 20 times the pipe diameter. Table 2 lists the computed slurry velocity at the central point of the cross-section of 20 times the pipe diameter under different grid cells. We can see that the relative errors for coarse mesh and medium mesh are 0.40% and 2.24%, respectively. Therefore, the medium mesh of 203,490 cells was used for the numerical simulation of sand transport and deposition in multiphase flow pipelines considering the computational cost and accuracy.

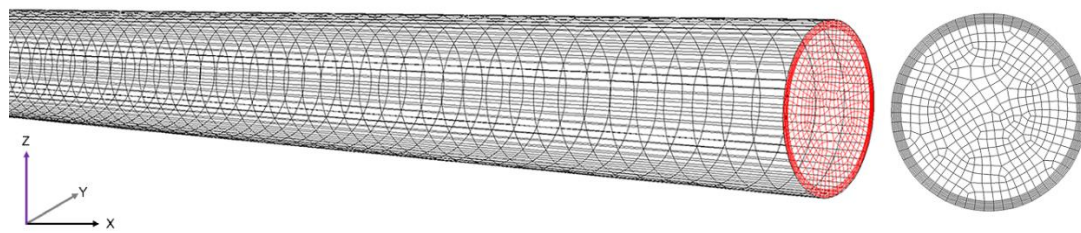


Figure 1. Pipe geometry and grid system for the numerical simulation.

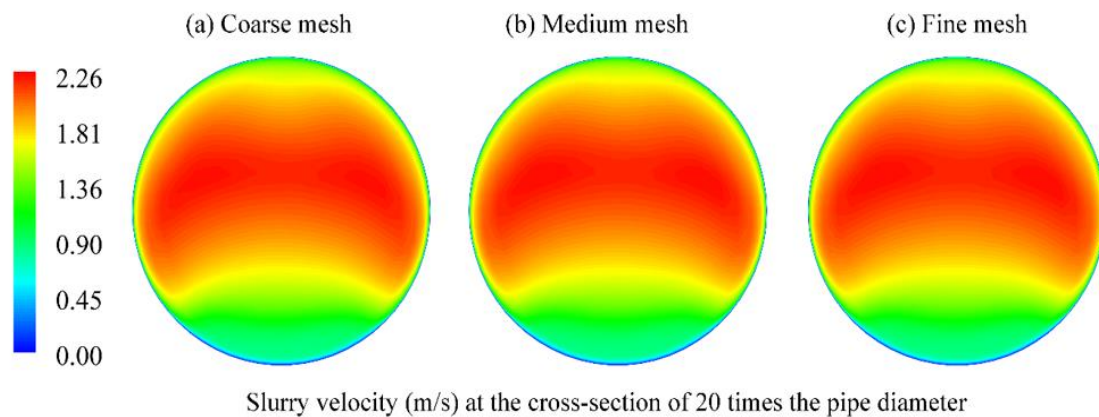


Figure 2. Contours of the slurry velocity under different grid cells for the numerical simulation of sand transport and deposition in multiphase flow pipelines.

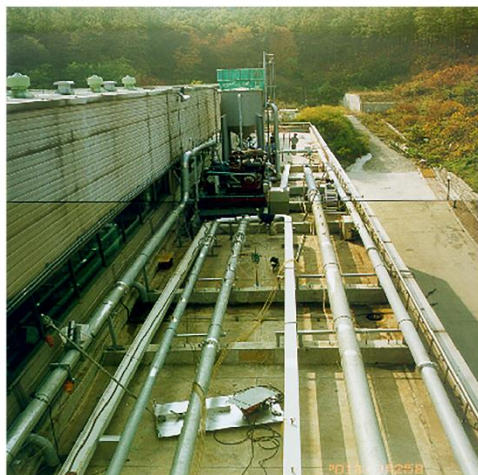
Table 2. Slurry velocity at the central point of the cross-section of 20 times the pipe diameter under different grid cells for the numerical simulation of sand transport and deposition in multiphase flow pipelines.

Grid Resolution	Slurry Velocity (m/s)	Relative Error (%)
Coarse mesh (121,080 cells)	2.0233	2.24
Medium mesh (203,490 cells)	2.0614	0.40
Fine mesh (466,820 cells)	2.0697	0

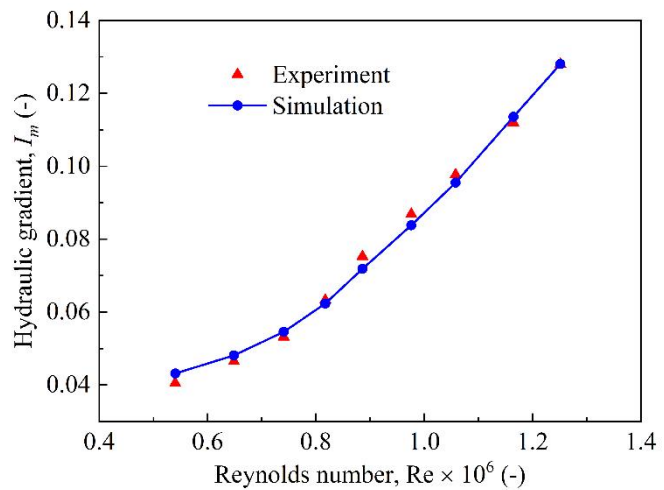
3. Results and Discussion

3.1. Model Validation

The developed numerical method for sand transport in multiphase flow pipelines was validated with experimental data [42]. Figure 3 shows the variation of the hydraulic gradient (I_m) along with the Reynolds number (Re) in the sand-slurry flow. The sand concentration is given by the volume ratio. The Reynolds number, Re , was calculated as $Re = vD\rho/\mu$, where D was the diameter of the pipe, v was the mean velocity of the slurry flow, ρ and μ were the density and the viscosity of the slurry flow, respectively. The hydraulic gradient, I_m , was defined as $I_m = \Delta p/(\rho gl)$, where p was the pressure, l was the pipe length, and g is the acceleration of gravity. It could be seen that our simulation agreed well with experimental data when the Reynolds number is from $(0.5\text{--}1.3) \times 10^6$. It demonstrated that the CFD method could accurately predict the sand transport in multiphase flow pipelines.



(a) Experimental set-up



(b) Experimental and numerical results

Figure 3. Effect of Reynolds number on the hydraulic gradient in sand-slurry flows (a) Set-up for experiments [32] and (b) comparison between experiments [32] and simulations.

3.2. Slurry Velocity

The sand content in multiphase flow pipelines is usually very small. However, the sand content of up to 30% is employed in this simulation for accelerated transport and deposition considering some extreme circumstances. Figures 4 and 5 present the liquid velocities at different cross-sections of multiphase flow pipelines in various slurry flows with the inlet velocity of 1.8 m/s. The detailed inputs for the numerical set-up are listed in Table 3.

Table 3. Detailed inputs for the numerical simulation of sand transport and deposition.

Numerical Inputs	Value
Diameter of the Pipe (mm)	200
Length of the Pipe (mm)	8000
Sand size (μm)	50, 300
Sand concentration (%)	5, 30
Inlet velocity of the slurry flow	1.8

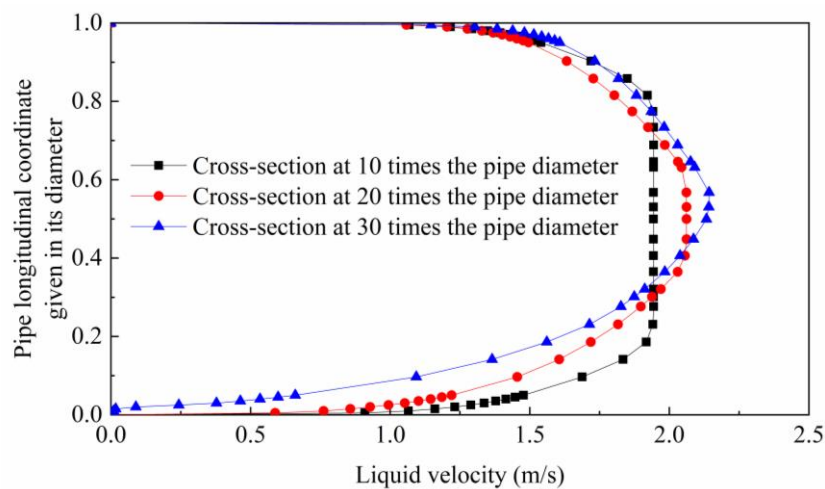


Figure 4. Liquid velocity at different cross-sections, $v_{in} = 1.8$ m/s, $d = 50 \mu\text{m}$, $c = 5\%$.

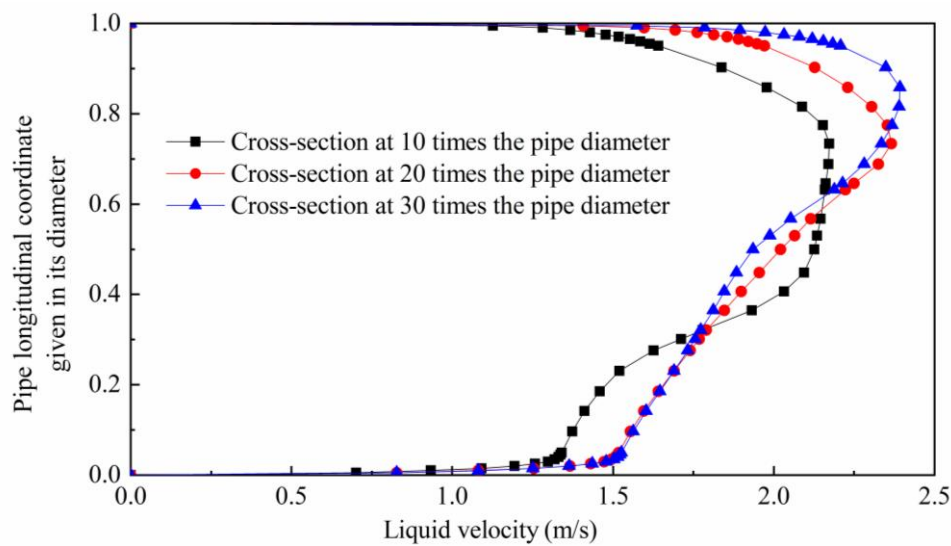
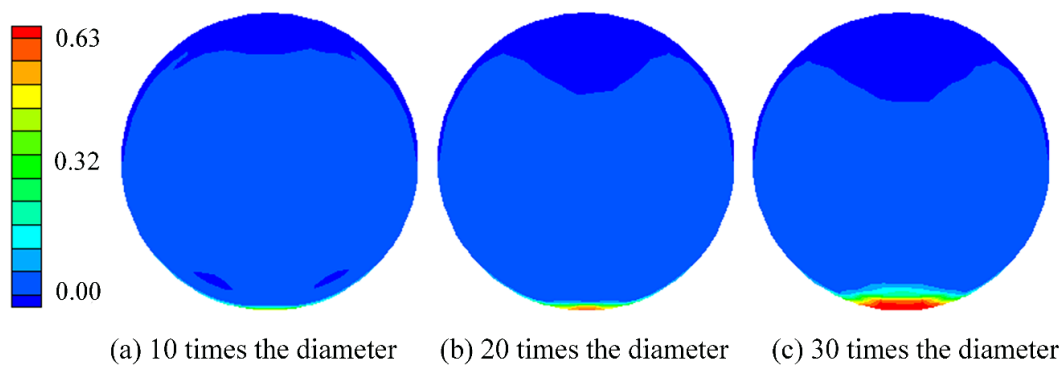


Figure 5. Liquid velocity at different cross-sections, $v_{in} = 1.8$ m/s, $d = 300$ μm , $c = 30\%$.

Under the condition of the lower concentration of the fine sand ($d = 50$ μm , $c = 5\%$), we could see from Figure 4 that the slurry velocities generally presented a uniform distribution in the turbulence area. Correspondingly, the vertical slurry velocity was symmetrical about the central axis. However, it could be seen from Figure 5 that the slurry velocities showed an extraordinarily nonuniform distribution in the higher concentration of the coarse sand ($d = 300$ μm , $c = 30\%$). In this higher concentration condition, the slurry velocities near the pipe top area were obviously larger than those close to the bottom area of the pipe. One of the major reasons was that the sands deposited in the pipe bottom in the slurry flow because of the large density difference between the liquid and the sand. In addition, the slurry velocities near the pipe wall area declined sharply due to the strong viscous shear stress in the turbulent boundary layer and non-slip boundary condition. This indicated that the liquids consumed more energy to carry these solid sands.

3.3. Sand Concentration

Figure 6 shows the sand concentration at different cross-sections away from the inlet of the pipeline. The initial computational condition included the sand concentration of 5%, the sand diameter of 50 μm and the slurry velocity of 1.8 m/s, respectively. It can be seen from these concentration contours that the sand can hardly settle in the pipe bottom within the distance of 10 times the pipe diameter from the pipe inlet (Figure 6a). After that, the sand begins to deposit as a result of the effect of the gravitational force along with the flow direction. In these simulation cases, the sand deposition was observed at the cross-section of 20 times the pipe diameter (Figure 6b). The deposition of the solid sand can be obviously found when the distance from the pipe inlet reaches 30 times the pipe diameter (Figure 6c). In other words, the thickness of the sand deposition is very small and it accordingly could be ignored, when the sand travelled less than 10 times the pipe diameter. Nevertheless, the deposition thickness reached approximately 10% of the pipe diameter, when the sand travelled about 30 times the pipe diameter in this simulation case.



Sand concentration at different pipe cross-sections of pipe length coordinate given in its diameter

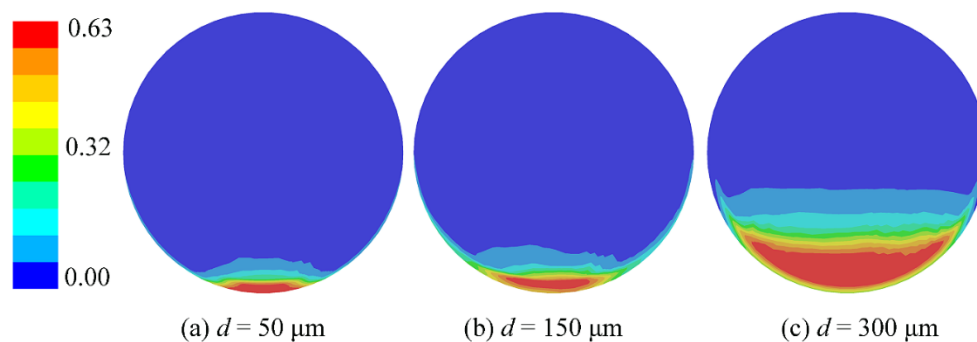
Figure 6. Sand concentration contours at different cross-sections of the multiphase flow pipeline.

3.4. Effect of the Particle Size

The effect of the particle size on the sand deposition was numerically simulated at the inlet velocity of 1.8 m/s with a sand concentration of 5%. The detailed inputs for the numerical set-up are listed in Table 4. The sand diameter is assumed to be 50 μm , 150 μm , and 300 μm , respectively. The results of the sand concentration are shown in Figure 7 at the cross-section of 30 times the pipe diameter. We can see that the height of the sand bed in the pipe bottom is small when the particle diameter is less than 50 μm . However, the height of the sand bed increases rapidly and it is even approximately equal to one-third of the pipe diameter when the sand diameter reaches 300 μm . Under this condition, the slurry flow cannot carry the coarse sand and correspondingly the severe deposition occurs in this low velocity of 1.8 m/s. It indicates that the sands cannot be carried by the liquid and the deposition will inhibit the flow assurance, especially for the subsea multiphase flow pipeline system.

Table 4. Detailed inputs for the numerical simulation of sand transport and deposition under the condition of different particle sizes.

Numerical Inputs	Value
Diameter of the Pipe (mm)	200
Length of the Pipe (mm)	8000
Sand size (μm)	50, 150, 300
Sand concentration (%)	5
Inlet velocity of the slurry flow	1.8



Sand concentration at the cross-section of 30 times the pipe diameter under different sand sizes ($v_{in} = 1.8 \text{ m/s}$, $c = 5\%$)

Figure 7. Sand concentration contours at the cross-section of 30 times the pipe diameter under the condition of different sand sizes ($v_{in} = 1.8 \text{ m/s}$, $c = 5\%$).

3.5. Effect of the Inlet Velocity

Figure 8 describes the effect of the inlet slurry velocity on the sand deposition and transport behaviour. The detailed inputs for the numerical set-up are listed in Table 5. The sand concentration is 5% and the sand diameter is 50 μm for the numerical condition. The inlet velocity is about 0.8 m/s, 1.8 m/s and 3.0 m/s for the simulation, respectively. The sand deposition is obviously observed in the pipe bottom while the inlet velocity is approximate 0.8 m/s. In this condition, the slurry velocity is not large enough to carry the solid sand, and correspondingly the deposition occurs. If the inlet velocity increases to 3.0 m/s, the sand can hardly deposit in the pipe bottom. Therefore, the slurry flow velocity is a major influence factor for sand deposition and transport.

Table 5. Detailed inputs for the numerical simulation of sand transport and deposition under the condition of different inlet velocities of the slurry flow.

Numerical Inputs	Value
Diameter of the Pipe (mm)	200
Length of the Pipe (mm)	8000
Sand size (μm)	50
Sand concentration (%)	5
Inlet velocity of the slurry flow	0.8, 1.8, 3.0

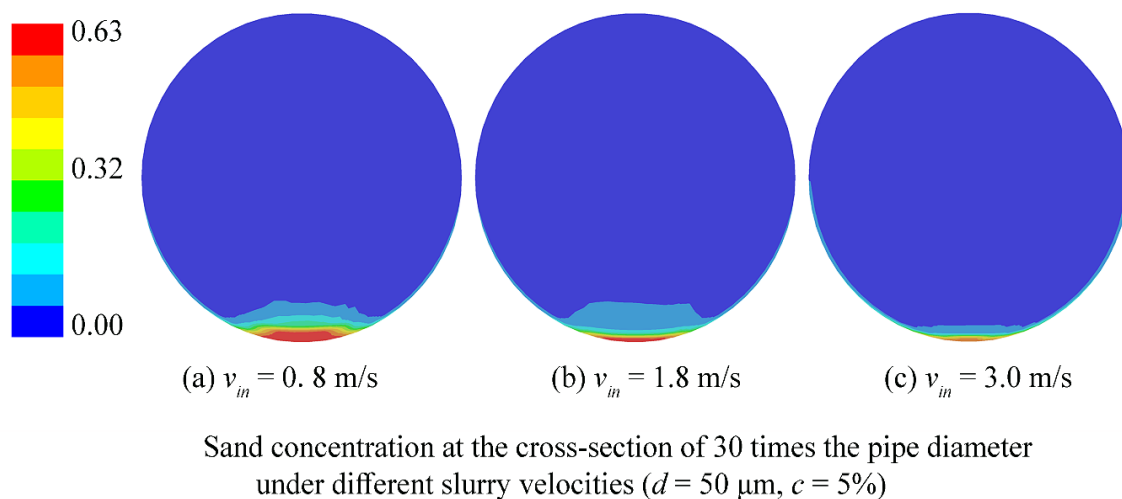


Figure 8. Sand concentration contours at the cross-section of 30 times the pipe diameter under the condition of different inlet slurry velocities ($d = 50 \mu\text{m}$, $c = 5\%$).

3.6. Discussion

Al-lababidi et al. [43] reported the experimental result of the sand transportation and deposition behaviour in a pipe of 0.05 m inner diameter under different sand concentrations and inlet velocities. If the inlet velocity was fixed at 1 m/s, most sands transported in the liquid core with the sand concentration of 0.00161%, while sand streaks were observed on the pipe bottom with the sand concentration of 0.0538%. This indicated that higher sand concentration resulted in the possibility of sand deposition in multiphase flows. Our numerical results in Figures 4 and 5 are in accord with these experimental observations. Furthermore, their experiments showed that increasing inlet velocity decreased the deposition of the sand in multiphase flows. For instance, the sand formed dunes on the bottom of the pipe and few sand particles moved on the top of the dunes with the sand concentration of 0.0108% when the inlet velocity was about 0.1 m/s. If the inlet velocity increased to 1 m/s, most sands transported in the liquid core at the same condition of the sand concentration. These experimental results are demonstrated in our simulations in Figure 8. Ofei and Ismail [44] numerically investigated the sand transport and deposition in multiphase flows in a pipe of 103 mm diameter. Their numerical

results showed that the maximum sand concentrations deposited on the pipe bottom were 15.1%, 21.5%, 25.8%, and 30.7% for the particle size of $d_p = 90 \mu\text{m}$, $150 \mu\text{m}$, $210 \mu\text{m}$, and $270 \mu\text{m}$, respectively. This illustrated that larger sand particles could accumulate on the pipe bottom and lead to the safety issue of the pipe operation. Our results in Figure 7 agree well with this trend of the particle size effect in point view of the qualitative analysis.

4. Conclusions

The Eulerian two-fluid model was developed to predict the transport and deposition behaviour of sands in multiphase flow pipelines. The numerical result shows that the slurry velocities at the vertical cross-section presented an extraordinarily non-uniform distribution in a higher concentration of the coarse sand compared to the condition of lower concentration of the fine sand. The sand could hardly settle in the pipe bottom at the cross-section of 10 times the pipe diameter, while the deposition was obviously observed at the cross-section of 30 times the pipe diameter. If the sand diameter was $300 \mu\text{m}$, the height of the sand bed would increase rapidly and it even approximately equal to one-third of the pipe diameter. For the sand diameter of $50 \mu\text{m}$ with a concentration of 5% slurry flow, the deposition was obviously observed in the pipe bottom with the inlet velocity of 0.8 m/s. The sand could hardly deposit in the pipe bottom if the inlet velocity increased to 3.0 m/s.

For the future work, we are carrying out the numerical and experimental studies on gas-liquid-solid multiphase flows in inclined pipelines, which will focus on the sand transport and deposition behaviour in this complicated pipeline system. The fluid flow analysis will be integrated to study the particle erosion issue, which is expected to contribute to the flow assurance of the complex oil and gas pipeline system.

Author Contributions: Conceptualization, Y.Y. and C.W.; formal analysis, Y.Y. and C.W.; writing—original draft preparation, Y.Y.; writing—review and editing, Y.Y., H.P., and C.W.; all authors read and approved the final manuscript.

Funding: This research was funded by the National Natural Science Foundation of China (No. 51606015).

Conflicts of Interest: The authors declare no conflict of interest.

References

1. Dotto, G.L.; dos Santos, J.N.; Rosa, R.; Pinto, L.A.A.; Pavan, F.A.; Lima, E.C. Fixed bed adsorption of Methylene Blue by ultrasonic surface modified chitin supported on sand. *Chem. Eng. Res. Des.* **2005**, *100*, 302–310. [[CrossRef](#)]
2. Danielson, T.J. Transient multiphase flow: Past, present, and future with flow assurance perspective. *Energy Fuels* **2012**, *26*, 4137–4144. [[CrossRef](#)]
3. Zorgani, E.; Al-Awadi, H.; Yan, W.; Al-Lababid, S.; Yeung, H.; Fairhurst, C.P. Viscosity effects on sand flow regimes and transport velocity in horizontal pipelines. *Exp. Therm. Fluid Sci.* **2018**, *92*, 89–96. [[CrossRef](#)]
4. Medlin, W.L.; Sexton, J.H.; Zumwalt, G.L. Sand transport experiments in thin fluids. In Proceedings of the SPE Annual Technical Conference and Exhibition, Las Vegas, NV, USA, 22–26 September, 1985.
5. Gao, H.; Guo, L.J.; Zhang, X.M. Liquid-solid separation phenomena of two-phase turbulent flow in curved pipes. *Int. J. Heat Mass Transf.* **2002**, *45*, 4995–5005. [[CrossRef](#)]
6. Kassai, M. Effectiveness and humidification capacity investigation of liquid-to-air membrane energy exchanger under low heat capacity ratios at winter air conditions. *J. Therm. Sci.* **2015**, *24*, 391–397. [[CrossRef](#)]
7. Doron, P.; Granica, D.; Barnea, D. Slurry flow in horizontal pipes—Experimental and modeling. *Int. J. Multiph. Flow* **1987**, *13*, 535–547. [[CrossRef](#)]
8. Gillies, R.G.; Shook, C.A. Concentration distributions of sand slurries in horizontal pipe flow. *Part. Sci. Technol.* **1994**, *12*, 45–69. [[CrossRef](#)]
9. Gillies, R.G.; Hill, K.B.; Mckibben, M.J.; Shook, C.A. Solids transport by laminar Newtonian flows. *Powder Technol.* **1999**, *104*, 269–277. [[CrossRef](#)]
10. Kaushal, D.R.; Tomita, Y. Solids concentration profiles and pressure drop in pipeline flow of multisized particulate slurries. *Int. J. Multiph. Flow* **2002**, *28*, 1697–1717. [[CrossRef](#)]

11. Kaushal, D.R.; Tomita, Y. Comparative study of pressure drop in multisized particulate slurry flow through pipe and rectangular duct. *Int. J. Multiph. Flow* **2003**, *29*, 1473–1487. [[CrossRef](#)]
12. Kaushal, D.R.; Sato, K.; Toyota, T.; Funatsu, K.; Tomita, Y. Effect of particle size distribution on pressure drop and concentration profile in pipeline flow of highly concentrated slurry. *Int. J. Multiph. Flow* **2005**, *31*, 809–823. [[CrossRef](#)]
13. Kaushal, D.R.; Tomita, Y. Experimental investigation for near-wall lift of coarser particles in slurry pipeline using γ -ray densitometer. *Powder Technol.* **2007**, *172*, 177–187. [[CrossRef](#)]
14. Duan, M.; Miska, S.Z.; Yu, M.; Takach, N.E.; Ahmed, R.M.; Zettner, C.M. Critical conditions for effective sand-sized solids transport in horizontal and high-angle wells. *SPE Dril. Com.* **2009**, *24*, 229–238. [[CrossRef](#)]
15. Najmi, K.; Hill, A.L.; McLaury, B.S.; Shirazi, S.A.; Cremaschi, S. Experimental study of low concentration sand transport in multiphase air–water horizontal pipelines. *J. Energy Res. Technol.* **2015**, *137*, 032908. [[CrossRef](#)]
16. Rice, H.P.; Fairweather, M.; Peakall, J.; Hunter, T.N.; Mahmoud, B.; Biggs, S.R. Measurement of particle concentration in horizontal, multiphase pipe flow using acoustic methods: Limiting concentration and the effect of attenuation. *Chem. Eng. Sci.* **2015**, *126*, 745–758. [[CrossRef](#)]
17. Roco, M.C.; Shook, C.A. Modeling of slurry flow: The effect of particle size. *Can. J. Chem. Eng.* **1983**, *61*, 494–503. [[CrossRef](#)]
18. Doan, Q.; Ali, S.M.; George, A.E.; Oguztoreli, M. Simulation of sand transport in a horizontal well. In Proceedings of the International Conference on Horizontal Well Technology, Calgary, AB, Canada, 18–20 November 1996; Richardson, Texas, USA, 1996.
19. Ling, J.; Skudarnov, P.V.; Lin, C.X.; Ebadian, M.A. Numerical investigations of liquid-solid slurry flows in a fully developed turbulent flow region. *Int. J. Heat Fluid Flow* **2003**, *24*, 389–398. [[CrossRef](#)]
20. Lin, C.X.; Ebadian, M.A. A numerical study of developing slurry flow in the entrance region of a horizontal pipe. *Comput. Fluids* **2008**, *37*, 965–974. [[CrossRef](#)]
21. Danielson, T.J. Sand transport modeling in multiphase pipelines. In Proceedings of the Offshore Technology Conference, Houston, TX, USA, 30 April–3 May 2007.
22. Wilson, K.C.; Sanders, R.S.; Gillies, R.G.; Shook, C.A. Verification of the near-wall model for slurry flow. *Powder Technol.* **2010**, *197*, 247–253. [[CrossRef](#)]
23. Messa, G.V.; Malin, M.; Malavasi, S. Numerical prediction of fully-suspended slurry flow in horizontal pipes. *Powder Technol.* **2014**, *256*, 61–70. [[CrossRef](#)]
24. Shi, D.P.; Luo, Z.H.; Zheng, Z.W. Numerical simulation of liquid-solid two-phase flow in a tubular loop polymerization reactor. *Powder Technol.* **2010**, *198*, 135–143. [[CrossRef](#)]
25. Kassai, M. Experimental investigation on the effectiveness of sorption energy recovery wheel in ventilation system. *Exp. Heat Transfer* **2018**, *31*, 106–120. [[CrossRef](#)]
26. Messa, G.V.; Malavasi, S. Improvements in the numerical prediction of fully-suspended slurry flow in horizontal pipes. *Powder Technol.* **2015**, *270*, 358–367. [[CrossRef](#)]
27. Hadinoto, K. Predicting turbulence modulations at different Reynolds numbers in dilute-phase turbulent liquid–particle flow simulations. *Chem. Eng. Sci.* **2010**, *65*, 5297–5308. [[CrossRef](#)]
28. Kaushal, D.R.; Thinglas, T.; Tomita, Y.; Kuchii, S.; Tsukamoto, H. CFD modeling for pipeline flow of fine particles at high concentration. *Int. J. Multiph. Flow* **2012**, *43*, 85–100. [[CrossRef](#)]
29. Soepyan, F.B.; Cremaschi, S.; Sarica, C.; Subramani, H.J.; Kouba, G.E. Solids transport models comparison and fine-tuning for horizontal, low concentration flow in single-phase carrier fluid. *AIChE J.* **2014**, *60*, 76–122. [[CrossRef](#)]
30. Dabirian, R.; Mohan, R.; Shoham, O.; Kouba, G. Critical sand deposition velocity for gas-liquid stratified flow in horizontal pipes. *J. Nat. Gas Sci. Eng.* **2016**, *33*, 527–537. [[CrossRef](#)]
31. Najmi, K.; McLaury, B.S.; Shirazi, S.A.; Cremaschi, S. The effect of viscosity on low concentration particle transport in single-phase (liquid) horizontal pipes. *J. Energy Res. Technol.* **2016**, *138*, 032902. [[CrossRef](#)]
32. Najmi, K.; McLaury, B.S.; Shirazi, S.A.; Cremaschi, S. Low concentration sand transport in multiphase viscous horizontal pipes: An experimental study and modeling guideline. *AIChE J.* **2016**, *62*, 1821–1833. [[CrossRef](#)]
33. Dabirian, R.; Arabnejad Khanouki, H.; Mohan, R.S.; Shoham, O. Numerical Simulation and Modeling of Critical Sand-Deposition Velocity for Solid/Liquid Flow. *SPE Prod. Oper.* **2018**, *33*, 866–878. [[CrossRef](#)]
34. Dabirian, R.; Mohan, R.; Shoham, O.; Kouba, G. Sand Transport in Slightly Upward Inclined Multiphase Flow. *J. Energy Res. Technol.* **2018**, *140*, 072901. [[CrossRef](#)]

35. Tebowei, R.; Hossain, M.; Islam, S.Z.; Droubi, M.G.; Oluyemi, G. Investigation of sand transport in an undulated pipe using computational fluid dynamics. *J. Pet. Sci. Eng.* **2018**, *162*, 747–762. [[CrossRef](#)]
36. Fajemidupe, O.T.; Aliyu, A.M.; Baba, Y.D.; Archibong-Eso, A.; Yeung, H. Sand minimum transport conditions in gas–solid–liquid three-phase stratified flow in a horizontal pipe at low particle concentrations. *Chem. Eng. Res. Des.* **2019**, *143*, 114–126. [[CrossRef](#)]
37. Leporini, M.; Marchetti, B.; Corvaro, F.; di Giovine, G.; Polonara, F.; Terenzi, A. Sand transport in multiphase flow mixtures in a horizontal pipeline: An experimental investigation. *Petroleum* **2019**, *5*, 161–170. [[CrossRef](#)]
38. Leporini, M.; Terenzi, A.; Marchetti, B.; Corvaro, F.; Polonara, F. On the numerical simulation of sand transport in liquid and multiphase pipelines. *J. Pet. Sci. Eng.* **2019**, *175*, 519–535. [[CrossRef](#)]
39. ANSYS Fluent. *18.0 ANSYS Fluent Theory Guide 18.0*; ANSYS Fluent: Canonsburg, PA, USA, 2017.
40. Yang, Y.; Zhu, X.; Yan, Y.; Ding, H.; Wen, C. Performance of supersonic steam ejectors considering the nonequilibrium condensation phenomenon for efficient energy utilisation. *Appl. Energy* **2019**, *242*, 157–167. [[CrossRef](#)]
41. Wen, C.; Karvounis, N.; Walther, J.H.; Yan, Y.; Feng, Y.; Yang, Y. An efficient approach to separate CO₂ using supersonic flows for carbon capture and storage. *Appl. Energy* **2019**, *238*, 311–319. [[CrossRef](#)]
42. Kim, C.; Lee, M.; Han, C. Hydraulic transport of sand-water mixtures in pipelines Part I. Experiment. *J. Mech. Sci. Technol.* **2008**, *22*, 2534–2541. [[CrossRef](#)]
43. Al-Lababidi, S.; Yan, W.; Yeung, H. Sand transportations and deposition characteristics in multiphase flows in pipelines. *J. Energy Res. Technol.* **2012**, *134*, 034501. [[CrossRef](#)]
44. Ofei, T.N.; Ismail, A.Y. Eulerian-Eulerian simulation of particle-liquid slurry flow in horizontal pipe. *J. Pet. Eng.* **2016**, *2016*, 5743471. [[CrossRef](#)]



© 2019 by the authors. Licensee MDPI, Basel, Switzerland. This article is an open access article distributed under the terms and conditions of the Creative Commons Attribution (CC BY) license (<http://creativecommons.org/licenses/by/4.0/>).